Vibrational spectra of amorphous clusters: Universal aspects

Gurpreet S. Matharoo, Subir K. Sarkar, and Akhilesh Pandey
School of Physical Sciences, Jawaharlal Nehru University, New Delhi 110 067, India
(Received 9 February 2005; revised manuscript received 4 May 2005; published 1 August 2005)

We have performed extensive numerical computations on the vibrational spectra of isolated amorphous clusters of medium to large size and containing one or two types of atoms. The interaction potential is also varied to study possible universality. For all the potentials and cluster sizes we find that the cumulative density of states can be described very accurately by the same functional form over a large central region of the spectrum. This functional form contains only one scale of frequency. We also find that the statistical fluctuations of the spectra are described by the Gaussian orthogonal ensemble of random matrices. For the largest clusters this is tested to a very high degree of precision in the central region and to a somewhat lower degree for most of the rest of the spectrum. We put forward a conjecture regarding the domain of the space of local minima of the potential energy function where universality with respect to the density of states function may be expected.

DOI: 10.1103/PhysRevB.72.075401 PACS number(s): 05.45.Mt, 63.50.+x, 61.43.Fs, 24.60.Lz

I. INTRODUCTION

An important component of the process of understanding amorphous states is the study of vibrational properties since these features are related to both structural and thermodynamic aspects of the material. This area of research has been pursued for several decades now but many key questions remain unanswered. To a large extent this is due to the difficulties arising out of the inherent nonlinearity of the problems. However, over the last few years, important progress has been made—sometimes following leads given many years ago.[1–26] One key ingredient in this development has been the renewed emphasis on a systematic study of the inherent structures which are the configurations corresponding to the local minima of the potential energy function used to describe the interactions between the constituent particles of the system. This is in contrast to some studies in which explicit models are made for both the geometry of the disordered state and the nature of the interaction. Thus, these investigations involving inherent structures have relegated the task of modeling to the more basic level of interparticle interactions. Once a choice is made for the interactions all the disordered inherent structures that can be generated from it are potential candidates for the geometry of the frozen amorphous state. Hence, the importance of a thorough study of the geometry, dynamics, and thermodynamics of the inherent structures in the understanding of amorphous systems is obvious. However, since the local minima depend on the choice of the interaction potential, presence of an element of universality is essential to make the conclusions generally relevant and to make comparisons to experimental results possible—unless the potential is derived from *ab initio* calculations. In this paper we present some such universal aspects of the vibrational spectra of model potentials for highly disordered states. Computations are done here for medium to large isolated clusters but some of our most important results are expected to become exact only in the bulk system limit. Calculation of vibrational frequencies is done by solving a suitable eigenvalue problem involving the Hessian matrix of the potential energy function corresponding to the inherent structure. Since we are dealing with disordered configurations it is natural that there is an element of randomness in this matrix and thus concepts familiar in the context of random matrix theory play a role in the way we describe the statistical fluctuations of the spectra—as has been done in the quantitative description of many physical problems, including that of vibrational spectra, in recent times.[27–33]

Two of the key results that will be presented in this paper are the following: (i) universality in the form of the density of states (DOS) over a large central part of the vibrational spectrum, defined as region II later in the paper, and (ii) universality in the nature of the statistical fluctuations of the spectra. In the language of random matrix theory, we find that the spectral fluctuations are of the type characteristic of the Gaussian orthogonal ensemble (GOE) of random matrices. To check for universality we study different types of potential available from the literature. The number of particles in the cluster is varied to study the effect of system size. We also address two general questions pertaining to the domain of universality for the density of states: (i) Which region of the space of all amorphous local minima can be expected to show universal properties? and (ii) for the region selected according to this criterion, does universality apply to the whole of the vibrational spectrum or only to a large part of it?

It is important to note here that a necessary condition for the universality of the density of states, even if over only a large part of the spectrum, is the disappearence of material-specific features as one goes from the crystalline state to highly disordered states. An understanding of how this happens in general was provided in an early work by Rehr and Alben.[5] In this picture the computation of the vibrational spectrum of a disordered system involves two steps. The first step is the construction of the geometry of the disordered configuration around which the vibration takes place. In the second step one constructs a model of vibration in which all pairs of elements within a suitable distance of each other are connected by linear springs—the spring constant for every such spring being, in general, a well-defined function of the distance between the pair of elements it connects. Even if

this spring constant is the same for every pair many of the features of the crystalline spectrum will be eliminated purely due to positional disorder and consequent change in the *connectivity* pattern compared to the ordered state. Thus this "topological disorder" will typically result in the survival of broad features since even disordered states have *local* geometry which is not very unlike that of the crystalline state. Now if we consider a situation in which the spring constants do depend on the distances between pairs through a sufficiently smooth function, disorder in pair separation will effectively generate another source of smearing of time scales of vibration. The actual magnitude of this effect will depend on how strongly the spring constant varies with distance (quantified by the third derivative of the pair potential). This is referred to as "quantitative disorder" and when this is increased progressively it will eventually remove all traces of even the broad features that survived topological disorder—leaving a spectrum with just one broad peak but otherwise featureless. Absence of features, however, does not automatically imply the presence of universality in the density of states. Universality is an additional and nontrivial property that our work suggests.

This paper is organized as follows. In Sec. II we describe the various potentials used by us. The methodology of the investigation and some related data are also presented in detail. Section III contains the results on single-component clusters with three different types of potentials. Results on binary mixtures are given in Sec. IV. In Sec. V we address issues regarding the domain of universality. Reference to some recent experiments on bulk glassy systems[34] is also made here in the light of our observations on universality. This is followed by discussion and conclusions. A brief account of some of the results reported here has already been published.[30]

II. METHODOLOGY

For our study of clusters in three dimensions we have used four different types of potentials. They are the Lennard-Jones (LJ), Morse, Sutton-Chen, and Gupta potentials. The explicit forms of the potentials are as follows: (1) LJ: $4\Sigma_{j>i}(1/r_{ij}^{12}-1/r_{ij}^{6})$ with the factor of 4 omitted for calculation of vibrational frequencies; (2) Morse: $\Sigma_{j>i}\{\exp[-2\alpha(r_{ij}-1)]-2\exp[-\alpha(r_{ij}-1)]\}$ with $\alpha=6$; (3) Sutton-Chen: $(1/2)\Sigma_{i=1}^{N}[\Sigma_{j\neq i}(1/r_{ij}^{9})]-\beta\Sigma_{i=1}^{N}\sqrt{\Sigma_{j\neq i}(1/r_{ij}^{6})}$ with $\beta=39.432$; and (4) Gupta: $\Sigma_{i=1}^{N}\{A\Sigma_{j\neq i}\exp[-p(r_{ij}-1)]\}-\Sigma_{i=1}^{N}\sqrt{\Sigma_{j\neq i}\exp[-2q(r_{ij}-1)]}$. Here N is the number of particles in the cluster and r_{ij} is the distance between particles i and j. The value of the parameter β for the Sutton-Chen potential is the one that describes nickel. Parameters of the Gupta potential have been varied to make it applicable to either nickel or vanadium.[35,36] The interesting point to note about these four potentials is that the expressions for the LJ and Morse types are of the form of sums over pairs of particles whereas those for the Gupta and Sutton-Chen types, used for describing metallic clusters, have many-body terms in them. For LJ clusters some results of the present investigation have already been published.[30]

Before the vibrational spectrum can be calculated, the configuration about which the vibration takes place needs to be known. These configurations can be any of the inherent structures of the potential in question and there are several methods available to generate them. We have used the method of homotopy minimization in which a local minimum for a function V is found by minimizing a sequence of functions of the form $\theta V+(1-\theta)U$ where U is a suitably chosen simple function. θ is changed from zero to one in a finite number of steps (about 20 in practice) and for each value of θ the initial guess for the configuration is the minimizing configuration for the previous value of θ.[37] In the first step the initial guess is a compact but random configuration. For the number of particles that we are dealing with, this method generates, in one trial, one of the higher-energy local minima with disordered geometry. With change in the random initial condition different local minima are produced. The number of distinct high-energy local minima that can be generated is, for all practical purposes, limitless for the system sizes we consider. But given the relatively small number of trials we are constrained to use, the energies produced for a given potential and for a given number of particles lie in a rather narrow range. Once an inherent structure is produced one computes the corresponding Hessian matrix and subsequent steps for computing the normal mode frequencies are standard. In this paper, unless stated otherwise, densities and fluctuation properties will always be computed for the *squares* of the vibrational frequencies (which are obtained as a result of solving a suitable eigenvalue problem). This has no effect on any of the conclusions drawn. For a particular inherent structure, we denote the elements of the eigenvalue spectrum (arranged in an increasing order) by $\lambda(i)$ with $i=1,2,\ldots,3N$. The first six of them will be identically equal to zero as a consequence of the translational and rotational symmetries of the potential. Characterization of the remaining nonzero eigenvalues is done by defining the mean local density as well as fluctuation around it. If we consider the spacing between two nearest neighbors in a spectrum then the variation of this spacing across the spectrum can be described as the sum of a component that changes rather smoothly and one that fluctuates very strongly—even between two adjacent pairs. The inverse of the first part is called the density of states and is an object of great physical interest since it is directly measurable through several experimental techniques and has immediate bearing on various physical properties of materials. Here we denote the DOS by $g(\lambda)$. As we will see later, an accurate knowledge of this function is also of crucial importance in doing a quantitatively precise analysis of the fluctuation aspects of the spectrum. Unfortunately, an analytic determination of $g(\lambda)$ is rarely possible and that is also true in our case. Starting from an eigenvalue spectrum obtained numerically we extract the DOS through the procedure described next.

Let $H(\lambda)$ be the number of eigenvalues less than or equal to λ and let $S(\lambda)$ be a sufficiently smooth function that passes through the staircase function H in the best-fit sense. Given the $H(\lambda)$ function resulting from a specific eigenvalue spectrum, $S(\lambda)$ is in practice constructed by first generating a suitable function space through a combination of various el-

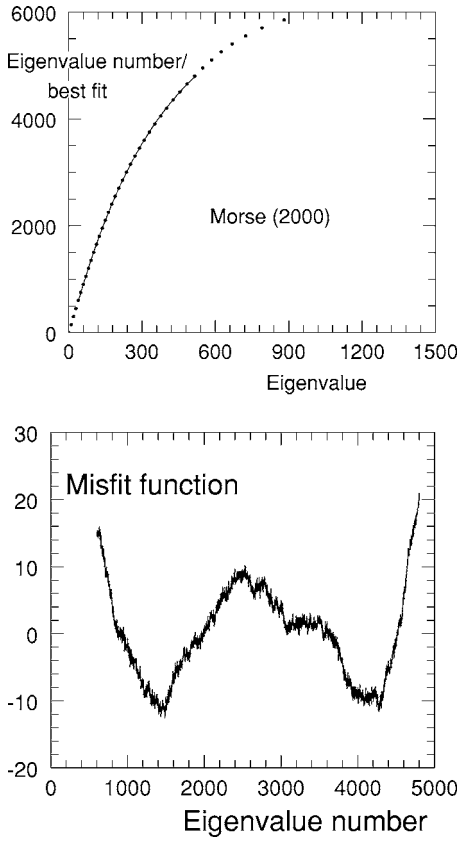

FIG. 1. (a) Filled circles: Eigenvalue (λ) vs eigenvalue number plot of a complete spectrum (Morse potential with $N=2000$). Some data points have been removed for clarity. Continuous line: Best-fit curve obtained after removing bottom 10% and top 20% of the spectrum. (b) Misfit function in the region of best fit for the same spectrum.

ementary functions and then performing an optimal fit in this space. The numerically determined DOS function is simply the derivative of this best-fit $S(\lambda)$. The first major result of this paper is contained in the following statement: Excluding relatively small regions (about 10–15 % of the levels) at each end of the spectrum, $S(\lambda)$ can be approximated extremely well by a function of the *form* $D(\lambda)=a-b\exp(-c\lambda)$. This is true of all the spectra of all the potentials we have studied. A measure of how well the best-fit $D(\lambda)$ approximates $S(\lambda)$ can be constructed by defining the misfit function $m(i)\equiv i-D(\lambda(i))$. Within the domain of the fit, let m_{max} be the maximum absolute value of this misfit function as calculated for the best-fit values of the adjustable parameters (a, b, and c) in the fitting function D. Then, m_{max} divided by the number of eigenvalues within the domain of the fit constitutes a proper measure of the accuracy of the approximation. We find that this quantifier stays at the level of one in 100 or less. Figure 1(a) provides a demonstration of this high accuracy of fit in a typical case. Figure 1(b) shows the misfit function for the same spectrum.

For a given type of potential, the DOS function $g(\lambda)$ should have the structure $Nf(\lambda)$ in the large-N limit. Here $f(\lambda)$ is a function that is independent of the number of particles but will, in general, depend on the energy per particle for the particular local minimum under consideration. With the kind of approximation we are using $g(\lambda)/N=(bc/N)\exp(-c\lambda)$. Thus the scales of λ and the normalized density of states are set by c and bc/N, respectively, both of which will depend on the specific local minimum. However, since we are generating minima only in a narrow energy range for a given potential and for a given number of particles, fluctuation of these two parameters of the DOS should be small—if we assume, as is conventional, that the energy of the inherent structure is the only parameter that controls the DOS function. Data in Table I on the values of the mean and standard deviation of c and bc/N show that this is indeed the case. In all cases the standard deviation decreases with increase in N. In the same limit the mean values appear to converge to nonzero values suggesting the existence of a well-defined DOS function in the large-system-size limit. Although we have no direct control over the energy of the inherent structure produced, this apparent convergence also suggests that the algorithm used ensures that the energy per particle indeed converges in the large-N limit (to a value on which we have no *a priori* control). It should be mentioned here that in our analysis of the central part of the spectrum we have consistently excluded the lowest 10% and the highest 20% of the data to get a fit that is of the quality mentioned earlier. We call this large central range "region II." The spectral regions below and above this range are referred to as "region I" and "region III," respectively. Data for these two relatively small regions have also been analyzed in ways that will be described later in the paper.

Statistical fluctuations of the eigenvalue spectra are analyzed using the procedures established in the theory of random matrices.[30–33] First of all, the raw spectrum of eigenvalues is transformed into an "unfolded" spectrum by using the map $s(i)\equiv S(\lambda(i))$. The unfolded spectrum thus generated derives its name from the fact that the smooth part of the DOS for these transformed eigenvalues is unity everywhere in the spectrum. It is this transformation that makes it possible to compare the fluctuation characteristics of two different spectra or two different parts of the same spectrum. Also, if there is reason to believe that in some situation all members of a set of spectra have the same kind of statistical fluctuation the information available from all the spectra can be combined to improve the statistics of the analysis. This is permissible only after the unfolding. Thus, for the purpose of analysis of fluctuations, spectrum will always mean unfolded spectrum. For a given potential and a given size of the cluster we generate a chosen number of local minima (in a narrow range of energy) and for every local minimum we derive the unfolded spectrum—bearing in mind that the transformation from the raw spectrum to the unfolded one is effected by the $D(\lambda)$ function with the parameters of D being the best fit values of a, b, and c for *that particular spectrum*. On this collection of unfolded spectra we perform the following statistical analysis: (i) Calculate the distribution of nearest-neighbor spacing denoted by the function $p(s)$, and (ii) characterize the probability distribution of the random variable $n(r)$, the number of eigenvalues within a singly connected domain of width r selected randomly from within the spectrum, in terms of its variance $[\Sigma^2(r)]$, skewness $[\gamma_1(r)]$, and excess $[\gamma_2(r)]$.

TABLE I. Statistical properties of the parameters of the best-fit cumulative density-of-states function in region II, and variance of the normalized nearest-neighbor spacing.

		c		cb/N		s
Potential	Number of particles	Average	Standard deviation	Average	Standard deviation	Variance
Lennard-Jones	200	1.60×10^{-2}	6.80×10^{-4}	1.56×10^{-2}	4.02×10^{-4}	0.2844
	500	1.38×10^{-2}	4.49×10^{-4}	1.37×10^{-2}	2.18×10^{-4}	0.2844
	1000	1.26×10^{-2}	2.51×10^{-4}	1.27×10^{-2}	1.34×10^{-4}	0.2852
	2000	1.17×10^{-2}	1.51×10^{-4}	1.20×10^{-2}	8.19×10^{-5}	0.2854
Morse	200	3.63×10^{-3}	1.43×10^{-4}	3.65×10^{-3}	9.59×10^{-5}	0.2864
	500	3.21×10^{-3}	7.97×10^{-5}	3.29×10^{-3}	5.07×10^{-5}	0.2844
	1000	2.97×10^{-3}	5.50×10^{-5}	3.09×10^{-3}	3.29×10^{-5}	0.2857
	2000	2.78×10^{-3}	3.66×10^{-5}	2.95×10^{-3}	2.26×10^{-5}	0.2845
Sutton-Chen	100	1.74×10^{-4}	6.76×10^{-6}	1.71×10^{-4}	6.44×10^{-6}	0.2908
	200	1.65×10^{-4}	4.19×10^{-6}	1.65×10^{-4}	4.34×10^{-6}	0.2882
	300	1.60×10^{-4}	3.37×10^{-6}	1.62×10^{-4}	4.25×10^{-6}	0.2833
	400	1.58×10^{-4}	2.70×10^{-6}	1.61×10^{-4}	4.45×10^{-6}	0.2856
Gupta (Nickel)	100	1.96×10^{-2}	8.76×10^{-4}	1.86×10^{-2}	8.53×10^{-4}	0.2942
	200	1.71×10^{-2}	6.14×10^{-4}	1.63×10^{-2}	3.83×10^{-4}	0.2838
	400	1.49×10^{-2}	7.39×10^{-4}	1.46×10^{-2}	2.48×10^{-4}	0.2841

III. SINGLE-COMPONENT CLUSTERS WITH MORSE, GUPTA, AND SUTTON-CHEN POTENTIALS

In this section we present the data on the nature of statistical fluctuations in the spectra of the local minima obtained with Morse, Gupta (with parameter values applicable to nickel), and Sutton-Chen types of potentials. The maximum cluster sizes used with these three types are 2000, 400, and 400, respectively. The much smaller system sizes for the Gupta and Sutton-Chen cases is caused by the nature of the expressions of the potential energy which are not of the form of sums over pairs. Due to this very large enhancement in the requirement of computation time, system sizes as well as the number of minima generated for these two cases are substantially less than those for the Morse potential.

A. Region II

First we present the data for the central 70% (region II) of the spectra as mentioned in Sec. II. For all the three types of potentials, analysis of randomly picked individual spectra suggested that the spectral fluctuations are of the GOE type—although with poor statistics. To improve statistics we combine the information from all the unfolded spectra for a given system size and a given potential.

Figures 2(a)–2(c) show the distribution $p(s)$ of the normalized nearest-neighbor spacing (s) for the largest system size used with each potential. We also superimpose the predictions from the Wigner surmise $[p(s)=(\pi s/2)\times\exp(-\pi s^2/4)]$ and the exact predictions for the GOE in each case.[31] The difference between the two predictions is at the level of 1% or less but the statistics for the Morse case is good enough (of the order of 10^6 levels after combining the spectra) to suggest convincingly that our data follow the exact GOE prediction rather than Wigner's surmise. The agreement for the Sutton-Chen and Gupta cases with much lower statistics looks significantly worse. But even for these cases the calculated values of $p(s)$ are within permissible limits of statistical fluctuation. For reference, the absolute number of data points in the bin at the peak of the $p(s)$ curve is about 1200 and 2300 for the Gupta and Sutton-Chen cases, respectively—compared to about 19 000 for the Morse potential. Data on the variance of the nearest-neighbor spacing are available in Table I. Exact calculation for the GOE and the analysis of Wigner's surmise lead to the values of 0.286 and 0.273, respectively, for this quantity. Agreement of the computed values of variance with the exact GOE result, rather than with Wigner's surmise, is extremely good.

For reliable computation of $\Sigma^2(r)$, the variance of the number of levels within a window of length r placed randomly in the spectrum, special attention has to be paid to the quality of the procedure that leads to the construction of the unfolded spectrum. As mentioned in Sec. II the function $D(\lambda)$ is indeed a very close approximation to the ideal function $S(\lambda)$. However, as can be seen from Fig. 1(b), there is also a systematic mismatch between these two. Even though the amplitude of the mismatch is only of the order of 1% (or less) of the range of fit it is enough to render the calculation of the variance for larger window sizes quite meaningless. This is due to the following reason. The spectrum of the GOE is extremely rigid and the variance $\Sigma^2(r)$ grows only as $\ln(r)$ whereas the error caused by the mismatch between the ideal fitting function and the one actually used is proportional to r^2—with the proportionality constant increasing with the level of mismatch. This makes it imperative that the mismatch be reduced to the lowest possible level and should ideally contain only statistical fluctuations inherent in the

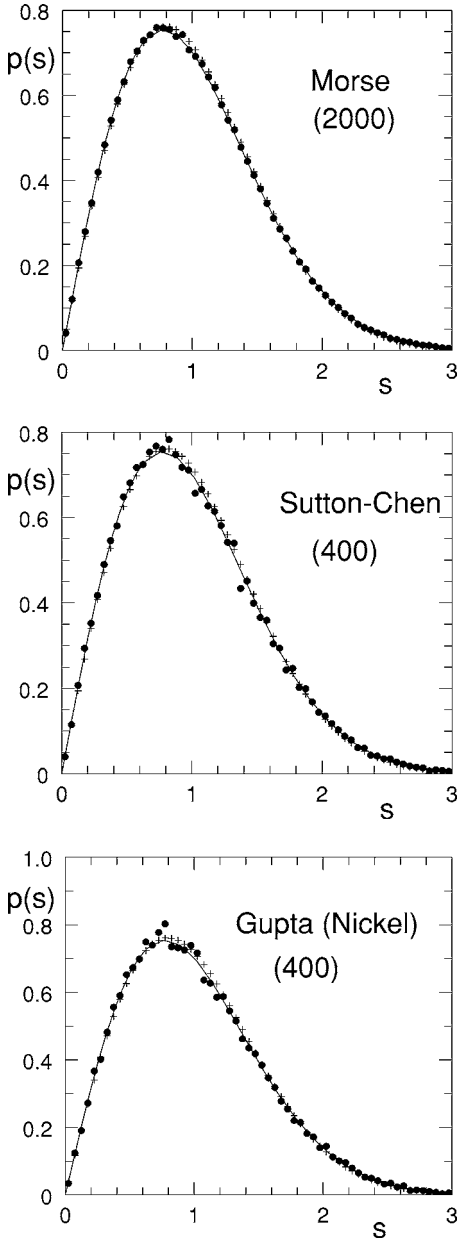

FIG. 2. Probability density $[p(s)]$ for normalized nearest-neighbor spacing (s) in the region II of the spectrum. Filled circles: our data. Crosses: Wigner's surmise for GOE. Continuous line: Exact prediction for the GOE. (a) Morse (N=2000), (b) Sutton-Chen (N=400), and (c) Gupta potential for nickel (N=400).

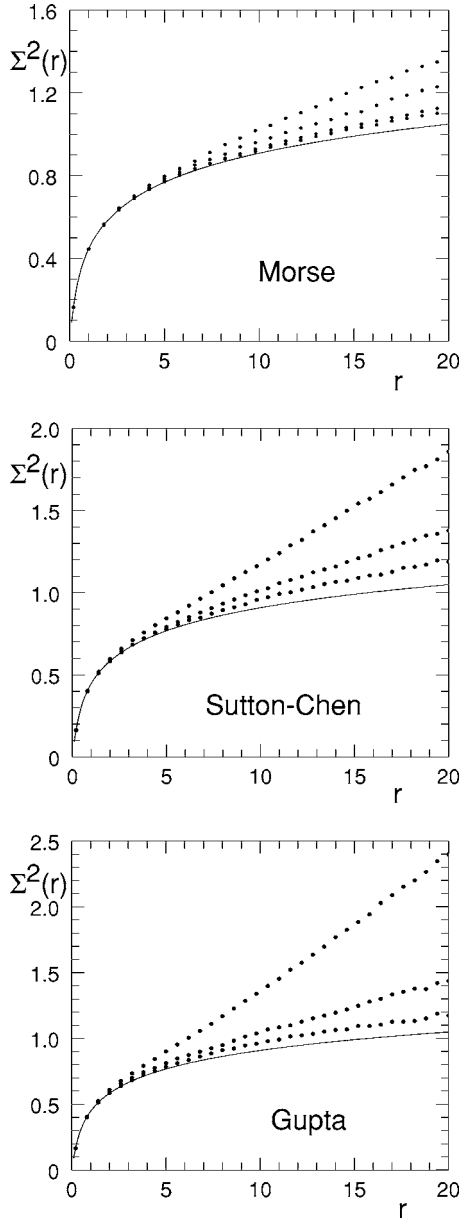

FIG. 3. Variance of the number of levels in intervals of length r plotted as a function of r for the region II of the spectrum. Continuous line: Prediction for the GOE. Filled circles: Our data. Number of particles (N) increases from top to bottom in each figure. (a) Morse with N=200, 500, 1000, and 2000; (b) Sutton-Chen with N=100, 200, and 400; and (c) Gupta potential for nickel with N =100, 200, and 400.

GOE spectrum. To accomplish this we construct a correction to the dominant fitting function $D(\lambda)$ by first eliminating from further consideration the regions in a spectrum where the mismatch function has rather irregular behavior and then fitting, in each of the remaining (typically two or three) relatively regular regions, quadratic functions to the mismatch function. Correcting $D(\lambda)$ by these quadratic functions leads to the desired unfolding functions. For a given value of r we combine the data for $n(r)$ from all the subregions of all the spectra for a given system size and potential before calculating $\Sigma^2(r)$, $\gamma_1(r)$, and $\gamma_2(r)$.

Figures 3(a)–3(c) show the data for $\Sigma^2(r)$ in the Morse, Sutton-Chen, and Gupta cases, respectively. In each figure data for several values of N are included to show the trend of variation with system size. In all cases the general trend is that the agreement between the computed data and the GOE prediction improves with increasing system size. A limitation of the procedure that we have actually used to compute variance here is that the subdomains into which every spectrum has been divided to avoid irregular regions contain eigenvalues with the *same* set of indices for all the local minima for a given potential and a given system size. Although the broad

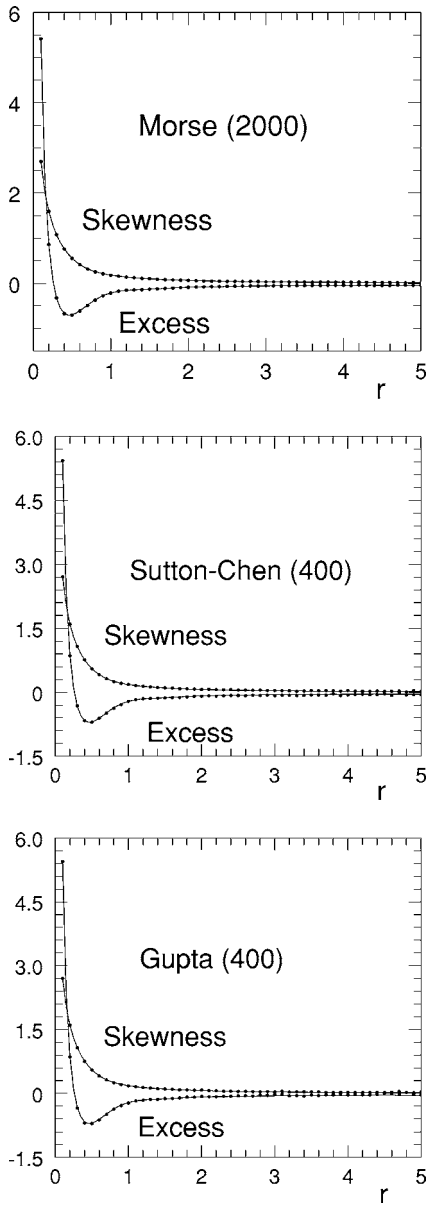

FIG. 4. Skewness and excess parameters of the distribution of $n(r)$, the number of levels in interval of length r, plotted as a function of r for the region II of the spectrum. Filled circles: Our data. Continuous lines: Predictions for GOE. (a) Morse with $N=2000$; (b) Sutton-Chen with $N=400$; and (c) Gupta potential for nickel with $N=400$.

contour of the misfit function is the same for every spectrum, exact locations of the irregular regions do vary somewhat from spectrum to spectrum. This simplification of the analysis is made due to the very large number of spectra that we are dealing with. However, in the case of the Lennard-Jones system with 2000 particles we have performed the analysis with spectrum-specific choice of subdomains. The resulting data for $\Sigma^2(r)$ are in practically overlapping agreement with the GOE prediction all the way up to $r=20$. Finally, we show the data for the excess (γ_1) and skewness (γ_2) parameters in Figs. 4(a)–4(c) along with the corresponding GOE predictions. It should be mentioned here that the predictions for skewness and excess parameters have been calculated by using a large ensemble of 500×500 matrices drawn from the Gaussian orthogonal ensemble. For each potential we display only the data for the largest system size since there is very little variation with system size. Values of r beyond 5 are not included since both $\gamma_1(r)$ and $\gamma_2(r)$ are very close to zero anyway in this range. Up to $r=5$ the agreement between the GOE prediction and our numerical data is very close—even with rather small system sizes.

B. Regions I and III

Now we present the spectral statistics for the top 20% (region III) and the bottom 10% (region I) of the spectra for the LJ and Morse cases. It is for only these potentials that the largest system size we have used is sufficiently big. As a result there are a meaningfully large number of levels even in these relatively small segments. There are two reasons why the analysis for the two ends of the spectra are being performed separately. (1) Due to our inability to find a *single* functional form that describes the density of states over the *entire* spectrum sufficiently accurately we cannot carry out the process of unfolding for all the eigenvalues in a single step. (2) Calculation of the participation ratios for the eigenmodes indicates that the modes belonging to the central 70% are extended. As one approaches the top of the spectra, the modes get progressively more and more localized until they become completely localized at the very top. At the lowest end the eigenmodes are a mixture of both localized and extended types. Since prevailing wisdom suggests a direct connection between the localization properties and the nature of spectral fluctuations it makes sense to analyze these regions separately so that the possibility of mixing different types of spectral statistics can be avoided. For the functional form of the cumulative density of states that is required for unfolding of spectra we choose a quadratic function in region I since the domain of fit is rather narrow. For region III the fitting function has the same form as in region II but the best-fit parameter values are substantially different. To achieve an acceptable quality of fit we remove a further 1% of the spectrum from the bottom of region I and 5% from the top of region III. Since there is hardly any difference between the results for the LJ and Morse cases we present the data only for the latter. Figures 5 and 6 display the data for the nearest-neighbor spacing and $\Sigma^2(r)$, respectively. It can be seen that the closeness of the nearest-neighbor spacing distribution for regions I and III to the GOE prediction is essentially of the same level as that for region II—except for somewhat higher degree of scatter on account of poorer statistics. This implies that departure from GOE statistics, if any, is weak among the levels included even though some of them are relatively more localized. Thus, for the spectrum as a whole, any deviation from GOE statistics must be confined to a rather small fraction of the levels at the two extremes. Since these excluded fringes contain only a small number of levels it is not presently possible to perform a statistically meaningful analysis of fluctuations independently for these regions.

Inspection of the data for $\Sigma^2(r)$, however, reveals a much greater deviation from the GOE prediction compared to region II when larger values of r are considered. This may be

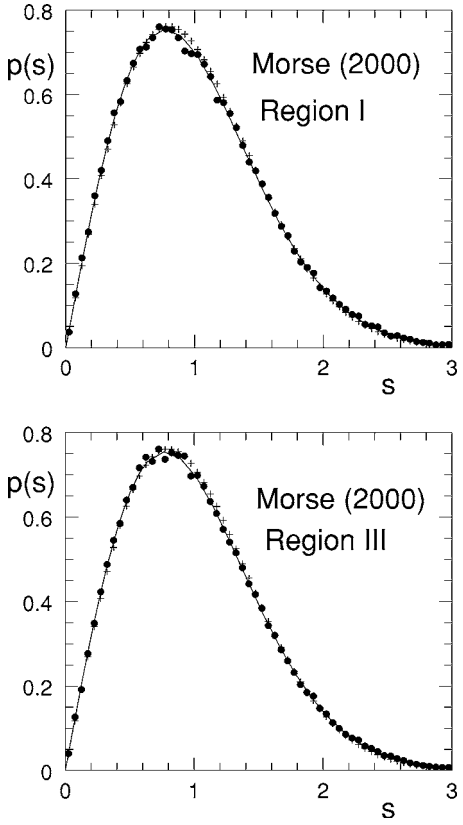

FIG. 5. Probability density $[p(s)]$ for normalized nearest-neighbor spacing (s), obtained with Morse potential $(N=2000)$, in the regions I and III of the spectrum. Filled circles: Our data. Crosses: Wigner's surmise for GOE. Continuous line: Exact prediction for the GOE. (a) Region I and (b) region III.

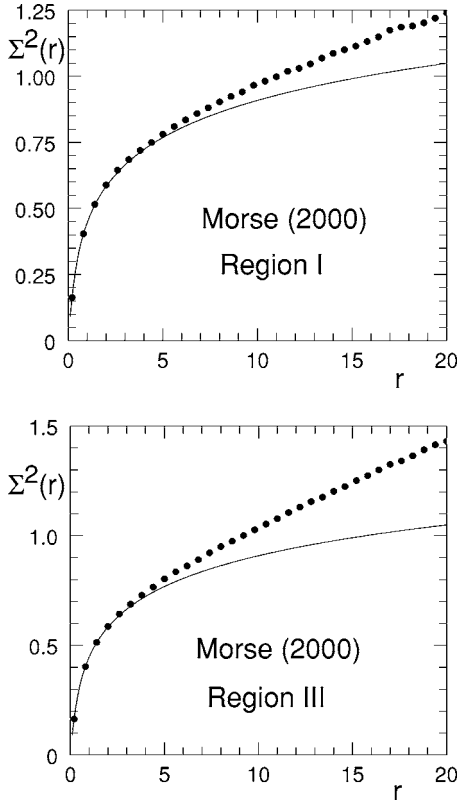

FIG. 6. Variance of the number of levels in intervals of length r plotted as a function of r for the regions I and III of the spectrum obtained with Morse potential $(N=2000)$. Continuous line: Prediction for the GOE. Filled circles: Our data. (a) Region I and (b) region III.

caused by a combination of two factors: (1) the quality of fit for the unfolding function (the nearest-neighbor spacing distribution is not so sensitive to the quality of fit) and (2) the genuine presence of some Poissonian statistics due to increasing localization at the two ends where regions I and III are located. However, it is difficult to estimate the relative contributions of the two factors—although the situation regarding the nearest-neighbor spacing would suggest that it is the quality of unfolding that is the dominant reason. A more careful analysis, with bigger system sizes, is required to settle these issues.

IV. BINARY MIXTURES

Results presented in Sec. III related to *single-component* systems. Given the hints of universality that are apparent in these data, it is obviously desirable to investigate whether these results are applicable to more general situations. Toward this goal we have studied binary LJ mixtures with various ratios of the numbers of the two types of particles, different system sizes, various rules for the construction of the LJ interaction parameters between the two species and with the masses of the two species being either the same or different. Here we present the data for only two cases. Denoting the two types of atoms by A and B, we take the ratio of the masses (m_B/m_A) to be 1.5. Let us recall that the complete expression of the LJ potential between two atoms of type P and Q, separated by the distance r, is given by $4\epsilon_{PQ}[(\sigma_{PQ}/r)^{12}-(\sigma_{PQ}/r)^6]$. Using this notation we take $\epsilon_{BB}/\epsilon_{AA}=0.5$ and $\sigma_{BB}/\sigma_{AA}=0.88$. $N_A+N_B=2000$ in both the cases. Here N_A and N_B denote the numbers of atoms of type A and B, respectively. However, the values of $N_A:N_B$, $\epsilon_{AB}/\epsilon_{AA}$, and σ_{AB}/σ_{AA} for the two cases are different. They are taken to be 50:50, $\sqrt{\epsilon_{BB}/\epsilon_{AA}}$, and $[1+(\sigma_{BB}/\sigma_{AA})]/2$, respectively, for case I (Lorentz-Berthelot rule) and 80:20, 1.5, and 0.8, respectively, for case II.[14]

Once again we find that the function $D(\lambda)$ provides an excellent fit to the cumulative density of states in region II—with the maximum absolute value of the misfit function not exceeding 1.5% of the range of fit for any of the local minima generated. Thus we can proceed with the process of unfolding as for the single-component systems. Figures 7–9 show the data for $p(s)$, $\Sigma^2(r)$, and skewness (plus excess), respectively for the two cases. The level of agreement with the GOE prediction is as good as in the case of a single-component LJ system of the same size for all aspects other than $\Sigma^2(r)$—where the disagreement for larger values of r is somewhat higher.

V. UNIVERSALITY OF THE DENSITY OF STATES

Until now we have been concerned almost exclusively with the fluctuational aspects of the spectrum in the language

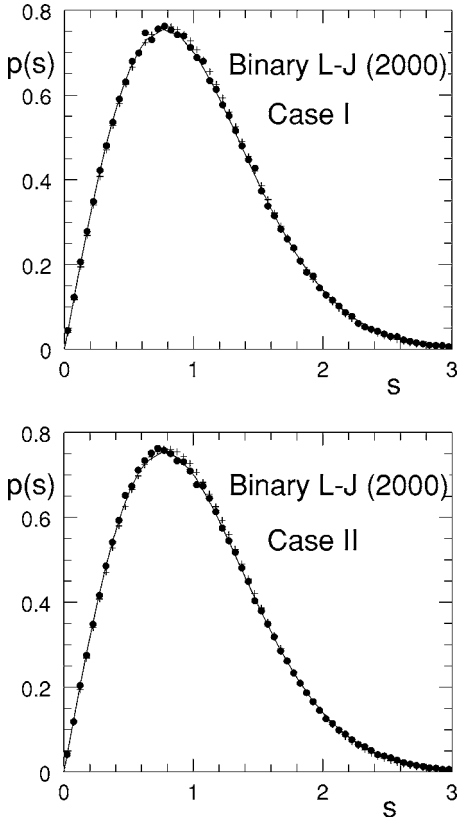

FIG. 7. Probability density $[p(s)]$ of normalized nearest-neighbor spacing (s) for the binary LJ mixture $(N=2000)$ in the region II of the spectrum. Filled circles: Our data. Crosses: Wigner's surmise for GOE. Continuous line: Exact prediction for the GOE. (a) Case I and (b) case II.

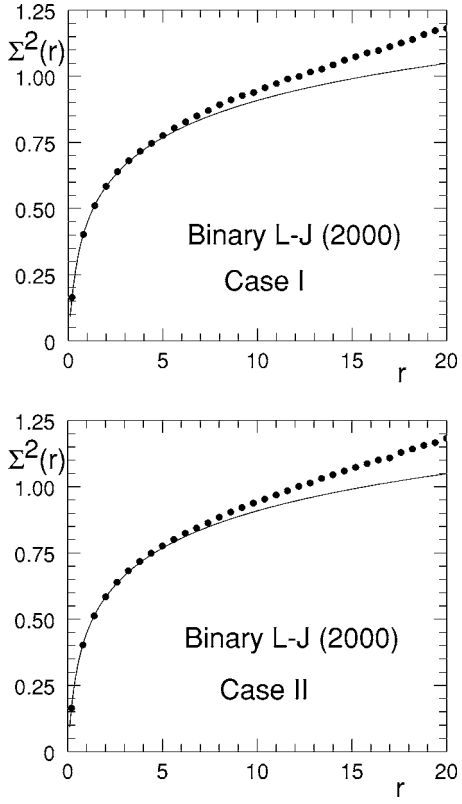

FIG. 8. Variance of the number of levels in intervals of length r plotted as a function of r for the binary LJ mixture $(N=2000)$ in the region II of the spectrum. Continuous line: Prediction for the GOE. Filled circles: Our data. (a) Case I and (b) case II.

of random matrix theories. We recall that the highly accurate unfolding of the spectrum, which is an essential first step of this kind of description, was made possible by the existence of a simple analytical formula $D(\lambda)$ that fitted the cumulative density of states very closely, *but not exactly*, over the region II of the vibrational spectra for all the amorphous local minima associated with the different types of potentials and the system sizes that we have studied. It is important to note that the function $D(\lambda)$ contains only a single scale $(1/c)$ for λ. This implies that all the DOS curves can be mapped into a single master curve to a good approximation in region II through a choice of frequency scale decided by the best-fit value of c. This demonstrates the existence of at least quasi-universality in the form of the density of states. In this section we investigate the issue of whether *rigorous* universality with respect to potential exists—at least in some well-specified situations. The first question we address here is the following. We are comparing the vibrational spectra of different potentials. For a given system size each potential has its own set of amorphous local minima in a broad and continuous range of energies and each such local minimum has an associated vibrational spectrum. Out of this range of possibilities for each potential which spectra should be considered while comparing different potentials? Establishing the existence of true universality with respect to potentials, if there is any, will require making the right choice of local minima also. We are not able to address this issue conclusively at this stage but we formulate a conjecture that is based on general theoretical considerations and plausibility. For the local minima that do satisfy the conditions of universality stated in this conjecture one may ask, is the universality applicable to the *entire* spectrum or only to a large part of it including region II? We analyze our existing data bank of vibrational spectra and present a likely scenario. In contrast to the previous sections here the density of states, unless otherwise stated, will refer to the vibrational frequency ω $(\lambda=\omega^2)$ since that is the quantity directly measured in laboratory experiments. We denote the DOS for ω by $G(\omega)$.

Our discussion here will assume that we are dealing with local minima corresponding to compact and connected clusters of a given shape (let us say spherical)—although in the large-size limit shape should be irrelevant. The existence of universality of the kind we are going to discuss here requires rigorous validity of the following assumptions which are consistent with our numerical data. (i) At least for system sizes that are large enough, the $G(\omega)$ function depends only on the energy and is not influenced by other details of the minima. (ii) The dependence of $G(\omega)$ on energy is smooth. Let us now order the elements of the set of all local minima according to energy. At the top of this energy-ordered family lie the completely amorphous structures which span a range of energies that is bounded above by, let us say, E_{max}. We know that the minima for which we have obtained the DOS curves satisfying approximate universality constitute a subset

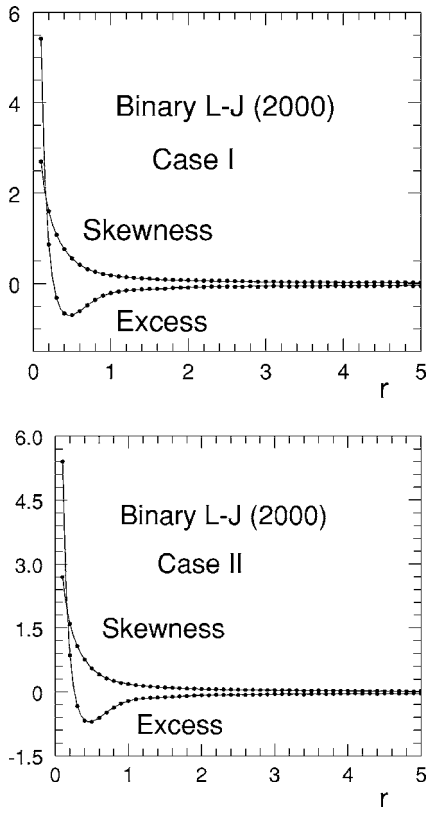

FIG. 9. Skewness and excess parameters of the distribution of $n(r)$, the number of levels in interval of length r, plotted as a function of r in the region II of the spectrum of the binary LJ mixture ($N=2000$). Filled circles: Our data. Continuous lines: Predictions for GOE. (a) Case I and (b) case II.

(within a narrow range of energies) of this family. However, we do not know how to locate E_{max} systematically and thus the location of the band of energies for our local minima with respect to E_{max} is uncertain. Our conjecture now is the following: As the size of the cluster increases towards the bulk limit, the DOS function corresponding to the local minima with the maximum possible energy (E_{max}) will approach a shape that is universal in the sense of being independent of potential. Should several universality classes exist, the asymptotic shape is decided by the class that the potential in question belongs to. Formulation of this conjecture is based on excluding the rather unnatural possibility that the evolution of the vibrational spectrum with the energy of the local minimum should saturate somewhere in the middle of the band representing completely amorphous states. Also, the lowest-lying minima (which lie well below this band of disordered states) correspond to quasicrystalline geometries with vibrational spectra that will clearly be potential specific. Thus, on grounds of continuity, we eliminate all local minima other than those at E_{max} as candidates for *true* universality. However, for the same reason of continuity, if the energy of a local minimum is close to E_{max} the associated vibrational spectrum will display a correspondingly close-to-universal shape. We presume this to be the explanation for the observation of near-universality in our numerical data. Finally, the energy per particle, the scale of frequency, and the normalized DOS for the highest-energy minima can reasonably be expected to have a well-defined bulk limit that is independent of shape.

We now address the question of whether shape universality is limited only to the large central part of the spectrum or is applicable to the whole of it. We presently have no theoretical tools to tackle this issue. Even a computational approach is beset by the difficulty that we are first of all required to identify the local minima with maximum possible energy—according to the conjecture stated above. Since we do not have access to a systematic method of doing this for clusters as large as the ones we are dealing with, we attempt to provide an approximate answer by assuming that the local minima that we have generated are not too far below E_{max} in energy. Stated in another way, we assume that the vibrational spectra that we have are close enough to that at E_{max} to ensure that our conclusions (which are qualitative anyway) based on the analysis of these somewhat lower-lying minima will be valid even at E_{max}, the point of true universality according to our conjecture. To proceed with the analysis we assume, to begin with, that the universality of shape applies to the whole of the spectrum and then check if our data are consistent with this assumption. To compute the universal shape of the vibrational spectra a proper choice of scale is needed for the individual frequencies in a spectrum. For a given spectrum a choice that would be consistent with our initial assumption is the average value of ω in *that* spectrum. Thus, we first rescale each frequency by this average. Next the DOS function for the rescaled ω is normalized so that the area under the DOS curve is unity. In Fig. 10(a) we display such normalized DOS functions for six different cases. The system size N is kept comparable (400 or 500) to minimize any possible discrepancy on this account. The six cases shown are (with the size of the cluster in parentheses) (i) single-component LJ (500), (ii) Morse (500), (iii) Sutton-Chen (400), (iv) Gupta for nickel (400), (v) Gupta for vanadium (400), and (vi) binary LJ mixture (500). For the binary LJ mixture the system parameters, other than size, are as in case I of Sec. IV. Before rescaling, the maximum values of ω for the six cases are around 16, 33, 150, 18, 5, and 32, respectively. Figure 10(b) shows similar data with $N=2000$ for (i) LJ, (ii) Morse, (iii) binary LJ, case I, and (iv) binary LJ, case II. Given the wide range of intrinsic frequency scales for the different potentials and mixtures, the conformity of Figs. 10(a) and 10(b) to the possibility of universality over the full spectrum would be considered to be strong in some instances. But considering that $D(\lambda)$ describes the cumulative DOS to within 1% in region II, which includes 70% of the whole spectrum, this apparent overlap is somewhat misleading. To show this we plot in Figs. 11(a) and 11(b) the data of Figs. 10(a) and 10(b), respectively, but with the scale of frequency taken to be $\sqrt{1/c}$—the frequency scale suggested by the functional form of $D(\lambda)$. Notice that the quality of overlap of the normalized DOS curves in region II (and the much smaller region I) is now much better. This suggests that universality may exist only in region II (and perhaps region I) and that the degradation in the quality of overlap all through the spectra in Figs. 10(a) and 10(b) is caused by the forced inclusion of region III where there is a breakdown of universality. Please note that in region III eigenmodes get progressively more localized as frequency increases. Density

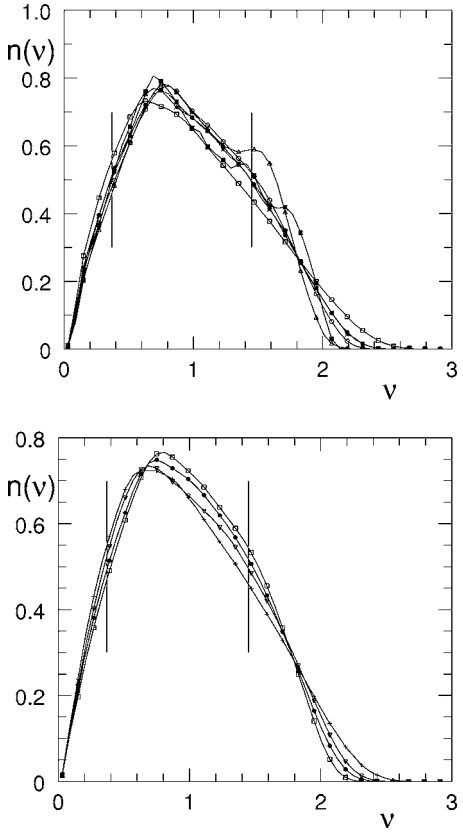

FIG. 10. Normalized density of states $[n(\nu)]$ for rescaled frequency (ν) with rescaling done by the average frequency of the corresponding spectrum. Vertical bars denote approximately the limits of region II. (a) Filled circles: LJ (500). Open circles: Morse (500). Open triangles: Sutton-Chen (400). Stars: Gupta for nickel (400). Filled squares: Gupta for vanadium (400). Open squares: Binary LJ (500). (b) Filled circles: LJ (2000). Open squares: Morse (2000). Crosses: LJ mixture, Case I (2000). Open inverted triangles: LJ mixture, case II (2000).

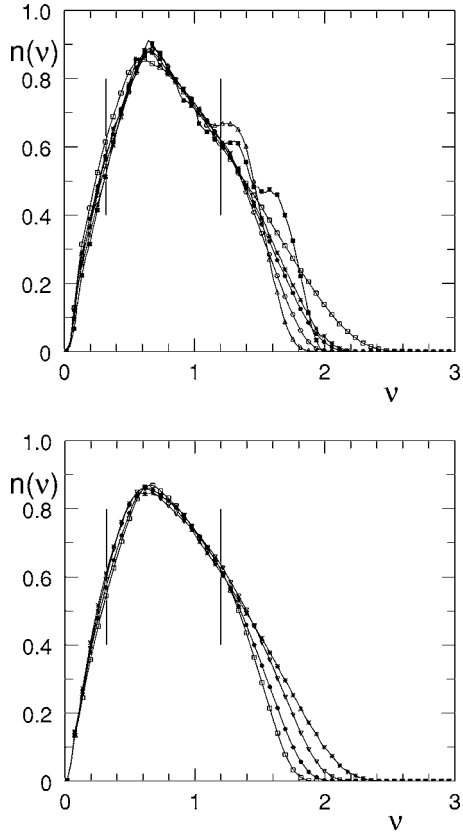

FIG. 11. Normalized density of states $[n(\nu)]$ for rescaled frequency (ν) with rescaling done by the best-fit frequency parameter of the region II of the corresponding spectrum. Vertical bars denote approximately the limits of region II. (a) Filled circles: LJ (500). Open circles: Morse (500). Open triangles: Sutton-Chen (400). Stars: Gupta for nickel (400). Filled squares: Gupta for vanadium (400). Open squares: Binary LJ (500). (b) Filled circles: LJ (2000). Open squares: Morse (2000). Crosses: LJ mixture, case I (2000). Open inverted triangles: LJ mixture, case II (2000).

of states for fully localized modes at the highest frequencies may reasonably be expected to be potential specific. Thus a plausible explanation of the absence of universality in the DOS function in region III might be that a crossover takes place across this region from the universality of region II to the potential specificity of the upper end of region III. However, while examining the validity of this explanation, the following point must be kept in mind: The spectral fluctuations in region III, excluding only the top 5% of the levels, are clearly of the GOE type for the largest system size we have studied and does not show the presence of any Poissonian contribution. It is not clear whether this observation and others connected with the issue of localization will remain unchanged as the system size keeps increasing toward the bulk limit. In particular the possibility that region III, the domain of violation of universality, will eventually start shrinking with increasing system size cannot be ruled out. In some cases exactly the opposite may also happen. To understand this possibility it has to be recognized that the presence of a surface in a cluster can be thought of as a topological disorder[5] as discussed in the Introduction and the smaller the cluster size the more severe is the effect. So when the cluster size increases, leading to a smaller fraction of the atoms being present at the surface, the smearing effect of the topological disorder will also be reduced and the single broad peak might split into more than one peak. We believe this to be the explanation for the presence of additional peaks which are small but still clearly visible in the Sutton-Chen spectrum for nickel and the Gupta spectrum for vanadium in Figs. 10(a) and 11(a). This may also provide clues to the limits of the universality class.

Recently, the suggestion of universality in the density of states for the vibrational spectra of highly disordered states[30] has also been made on the basis of data from laboratory experiments with a variety of glasses.[34] These experiments involve bulk systems and the constituents are more complex than in our case where position is the only degree of freedom. Thus there are additional complex spectral features present. However, data of the type presented in Fig. 3(b) and 3(c) of Ref. 34, when interpreted in the way it is done in that work, support the same concept of universality that we discuss in this paper. The functional form of the universal DOS function in the trans-boson-peak region put forward in Ref. 34 is different from that implied by our $D(\lambda)$ function. How-

TABLE II. Ratio of moments for various potentials, compositions, and system sizes.

Potential	Number of particles	$\bar{\lambda}$	$\bar{\lambda}^2/\bar{\lambda}^2$	$\bar{\lambda}^3/\bar{\lambda}^3$	$\bar{\lambda}^4/\bar{\lambda}^4$
Sutton-Chen	100	5644.5	1.6676	3.4641	8.1032
	200	5657.8	1.6513	3.3821	7.7913
	300	5677.3	1.6368	3.3139	7.5395
	400	5693.4	1.6286	3.2775	7.4116
Gupta (nickel)	100	56.9	1.8360	4.5041	13.0656
	200	61.7	1.8087	4.3018	11.9598
	400	66.3	1.7621	4.0328	10.7267
Gupta (vanadium)	400	7.9	1.7034	3.6336	8.7015
Morse	200	261.5	1.7452	3.9473	10.3628
	500	280.4	1.7063	3.7216	9.3429
	1000	291.6	1.6825	3.5934	8.7990
	2000	300.8	1.6634	3.4933	8.3869
Lennard-Jones (monatomic)	200	62.8	1.7968	4.2480	11.7732
	500	69.0	1.7621	4.0360	10.7592
	1000	72.7	1.7375	3.8950	10.1187
	2000	75.8	1.7148	3.7687	9.5627
Lennard-Jones (binary, case I)	500	195.8	1.9088	4.9043	14.9385
	1000	206.2	1.8798	4.7182	13.9731
	2000	214.7	1.8558	4.5728	13.2627
Lennard-Jones (binary, case II)	1000	376.6	1.7662	4.0473	10.7777
	2000	364.2	1.7684	4.0430	10.7030

ever, it does have only one scale of frequency which is a necessary condition of shape universality. We have verified that this alternative functional form also fits our numerical data quite closely. This should not be considered particularly surprising since the domain of fit is limited. The procedure used to test the suitability of the alternate functional form for our data is the following. In Ref. 34 the DOS function for ω is $G(\omega)=\alpha\omega^2\exp(-\beta\omega)$. For the cumulative density of states of ω this implies a functional form $I(\omega)=\text{const}-(2\alpha/\beta^3)[1+\beta\omega+(1/2)(\beta\omega)^2]\exp(-\beta\omega)$. Now we repeat the analysis described in Sec. II with λ and $D(\lambda)$ replaced by ω and $I(\omega)$, respectively. We find that the misfit function now has comparable or somewhat smaller amplitude than what is obtained with the combination of λ and $D(\lambda)$. This change, however, has no discernible quantitative effect on the analysis of fluctuations since any difference in the quality of unfolding due to the difference of functional form is compensated by the subsequent process of correction with the quadratic fit to the residue.

Finally, the universality of the DOS function can also be tested through a study of the various moments of frequency since the discrete but infinite collection of all moments carries the same information as the single but continuous DOS function. A random matrix type theory of universality is more likely to concentrate on those moments that can be defined for both λ and ω. However, since λ plays a more immediate role for theoretical calculations we will use only this variable here. Universality of the DOS in the present context implies the existence of a single scale for λ in the DOS function. Defining $R(n)=\langle\lambda^n\rangle/\langle\lambda\rangle^n$ for every positive integral value of n, it follows that $R(n)$ should be universal. In Table II we present the data on this ratio for $n=2$, 3, and 4 for the various systems we have studied. The first point to be noted here is the wide variation of the scale of frequency (represented by average frequency in the table) for the various systems. It extends over almost three decades. Second, as the order of the moment increases the higher-frequency domain becomes progressively more dominant in determining the ratio. Thus any deviation from universality in the numerical data for the high-frequency region will be reflected more and more in the moment ratios for higher order. The utility of the data presented in Table II should be evaluated with these factors in mind. We find, almost without exception, that $R(n)$ decreases gradually as the system size increases while keeping the value of n, the potential, and the composition fixed. However, convergence is weak. Comparison of the data for different types of potentials also shows that the pattern of convergence is not conclusive but it is also not inconsistent with the conjecture of universality at this level. Bigger system sizes are clearly required to clarify this issue.

VI. DISCUSSION AND CONCLUSIONS

In this paper we have presented numerical results on the universal nature of certain aspects of the vibrational spectra of amorphous clusters. They can be classified into three main categories: (i) universality of statistical fluctuations, (ii) universality of the density of states over the large central region of the spectrum, and (iii) analysis of the domain of

universality—both in the space of all local minima and within each spectrum. For the various potentials that we have used the quality of the numerical evidence regarding the first two types of results is quite convincing for both single-component systems and binary mixtures—as long as the explicitly stated limits are understood. However, since it is not possible to generalize the conclusions of any such numerical work, it will be desirable to derive these results analytically. This will help establish the limits of validity and perhaps classification into various universality classes. It may also shed light on the validity of the rather strong conjecture put forward in Sec. V. A further incentive toward this goal is provided by the experimental evidence of universality in the vibrational spectra of collective modes of several glassy materials that have been studied recently.[34]

Some amorphous systems are clearly beyond the scope of the present study. For example, materials in which bonding is at least partially directional will require the inclusion of degrees of freedom beyond just the positions of the atoms. There are also systems (e.g., gold) in which the smallest-sized clusters have amorphous states as the lowest-energy structures—as opposed to our systems where the amorphous states correspond to the highest-energy local minima. However, even for these materials, when the cluster size is sufficiently large, the normal relationship between order and energy is restored.[38]

One important aspect of our calculations is that the amorphous systems that we study have geometrical disorder that is generated naturally from the interactions and they do not involve any kind of modeling. Combined with the property of universality, this feature leads us to expect that our calculations will correspond directly with the observations in laboratory experiments. Thus analysis of the vibrational spectra obtained experimentally for various glassy materials can provide very important complementary strands in the examination of the theme of universality in the density of states.

As far as statistical fluctuations are concerned the numerical evidence in favor of the GOE type is exceptionally strong. However, it cannot be claimed that we have a satisfactory understanding of *why* it is so. It is true that the matrices that are diagonalized to get the spectra have some of the properties that are included in the definition of GOE. But it is not clear at this time why the correlations that are obviously present in the Hessian matrices turn out to be of no consequence. Clarification of this issue requires further study.

Verification of the presence of GOE statistics beyond model potentials will require a sufficiently precise and complete cataloging of at least parts of a spectrum. For laboratory experiments on clusters this goal poses a stiff challenge but some progress in this direction has been reported recently.[39] It is encouraging to note that the nearest-neighbor spacing distribution as well as the skewness and excess parameters are very close to the exact GOE predictions for a cluster size as small as 100. This brings the job of verification much closer to the realm of possibilities—especially with regard to *ab initio* calculations. For larger systems, the issue of resolution will obviously make impractical any attempt to obtain even a part of the vibrational spectrum. An alternative could be to look for the influence of the statistics on some thermodynamic properties. Unfortunately, at this time, we are not aware of any such effect.

In the absence of a convincing theoretical argument, evidence in favor of or against our conjecture regarding the domain of universality for the density-of-states function in the space of all amorphous local minima can still be produced, in principle, numerically for specific choices of potential. But that will require a methodological improvement in the way local minima are generated. It is necessary to have access to a systematic and practically feasible method that can generate the highest-energy minima for large clusters. In particular any claim of having generated such states must be accompanied by a proof that local minima with higher energies do not exist. The data bank generated by the present method suffers from uncertainty in this respect. The mapping of DOS curves with a large range of intrinsic frequency scales into an almost single curve in a broad range is strongly suggestive. But the discrepancies that still exist warrant further investigation—given the generality and wide physical ramifications of the theme of universality. In particular, laboratory experiments and *ab initio* calculations on a larger variety of systems would be helpful.

ACKNOWLEDGMENT

G.S.M. thanks CSIR, India, for financial support.

[1] G. Adams and J. H. Gibbs, J. Chem. Phys. **43**, 139 (1965).
[2] M. Goldstein, J. Chem. Phys. **51**, 3728 (1969).
[3] R. J. Bell, Rep. Prog. Phys. **35**, 1315 (1972).
[4] A. Rahman, M. J. Mandell, and J. P. McTague, J. Chem. Phys. **64**, 1564 (1976).
[5] L. V. Heimendahl and M. F. Thorpe, J. Phys. F: Met. Phys. **5**, L87 (1975); J. J. Rehr and R. Alben, Phys. Rev. B **16**, 2400 (1977).
[6] F. H. Stillinger and T. A. Weber, Phys. Rev. A **25**, 978 (1982); Science **225**, 983 (1984); F. H. Stillinger, *ibid.* **267**, 1935 (1995); S. Sastry, P. G. Debenedetti, and F. H. Stillinger, Nature (London) **393**, 554 (1998); S. Sastry, *ibid.* **409**, 164 (2001).
[7] C. A. Angell, J. Non-Cryst. Solids **131–133**, 13 (1991).
[8] F. J. Bermejo, J. Alonso, A. Criado, F. J. Mompeán, J. L. Martínez, M. García-Hernández, and A. Chahid, Phys. Rev. B **46**, 6173 (1992).
[9] V. A. Luchnikov, N. N. Medvedev, Y. I. Naberukhin, and V. N. Novikov, Phys. Rev. B **51**, 15569 (1995).
[10] K. Vollmayr, W. Kob, and K. Binder, J. Chem. Phys. **105**, 4714 (1996).
[11] Physica D **107**(2–4), (1997), special issue.
[12] B. Fultz, C. C. Ahn, E. E. Alp, W. Sturhahn, and T. S. Toellner,

Phys. Rev. Lett. **79**, 937 (1997); O. Pilla, S. Caponi, A. Fontana, M. Montagna, F. Rossi, G. Villani, L. Angelani, G. Ruocco, G. Monaco, and F. Sette, cond-mat/0209519 (unpublished); C. A. Tulk, D. D. Klug, E. C. Svensson, V. F. Sears, and J. Kastaras, Appl. Phys. A: Mater. Sci. Process. **74** (Suppl.), S1185 (2002); M. A. Parshin, C. Laermans, D. A. Parshin, and V. G. Melehin, Physica B **316–317**, 549 (2002); M. A. Ramos, C. Talón, R. J. Jiménez-Riobóo, and S. Vieira, J. Phys.: Condens. Matter **15**, S1007 (2003); N. V. Surovtsev, S. V. Adichtchev, E. Rössler, and M. A. Ramos, *ibid.* **16**, 223 (2004).

[13] W. Schirmacher, G. Diezemann, and C. Ganter, Phys. Rev. Lett. **81**, 136 (1998); Physica B **284–288**, 1147 (2000); P. Carpena and P. Bernaola-Galvan, Phys. Rev. B **60**, 201 (1999).

[14] W. Kob and H. C. Andersen, Phys. Rev. Lett. **73**, 1376 (1994); F. Sciortino, W. Kob, and P. Tartaglia, *ibid.* **83**, 3214 (1999).

[15] K. K. Bhattacharya, K. Broderix, R. Kree, and A. Zippelius, Europhys. Lett. **47**, 449 (1999).

[16] A. Cavagna, I. Giardina, and G. Parisi, Phys. Rev. Lett. **83**, 108 (1999); T. S. Grigera, V. Martín-Mayor, G. Parisi, and P. Verrocchio, *ibid.* **87**, 085502 (2001); T. S. Grigera, A. Cavagna, I. Giardina, and G. Parisi, *ibid.* **88**, 055502 (2002); T. S. Grigera, V. Martín-Mayor, G. Parisi, and P. Verrocchio, Nature (London) **422**, 289 (2003).

[17] S. Büchner and A. Heuer, Phys. Rev. Lett. **84**, 2168 (2000); R. A. Denny, D. R. Reichman, and J. -P. Bouchaud, *ibid.* **90**, 025503 (2003).

[18] W. Kob, F. Sciortino, and P. Tartaglia, Europhys. Lett. **49**, 590 (2000).

[19] T. B. Schrøder, S. Sastry, J. C. Dyre, and S. Glotzer, J. Chem. Phys. **112**, 9834 (2000).

[20] K. Broderix, K. K. Bhattacharya, A. Cavagna, A. Zippelius, and I. Giardina, Phys. Rev. Lett. **85**, 5360 (2000); L. Angelani, R. Di Leonardo, G. Ruocco, A. Scala, and F. Sciortino, *ibid.* **85**, 5356 (2000); P. Shah and C. Chakravarty, *ibid.* **88**, 255501 (2002).

[21] G. Ruocco, F. Sette, R. Di Leonardo, G. Monaco, M. Sampoli, T. Scopigno, and G. Viliani, Phys. Rev. Lett. **84**, 5788 (2000).

[22] S. N. Taraskin, Y. L. Loh, G. Natarajan, and S. R. Elliott, Phys. Rev. Lett. **86**, 1255 (2001).

[23] A. Cavagna, Europhys. Lett. **53**, 490 (2001).

[24] E. La Nave, S. Mossa, and F. Sciortino, Phys. Rev. Lett. **88**, 225701 (2002); S. Mossa, E. La Nave, H. E. Stanley, C. Donati, F. Sciortino, and P. Tartaglia, Phys. Rev. E **65**, 041205 (2002); S. Mossa, E. La Nave, P. Tartaglia, and F. Sciortino, J. Phys.: Condens. Matter **15**, S351 (2003).

[25] C. A. Angell, Y. Yue, L.-M. Yang, J. R. D. Copley, S. Borick, and S. Mossa, J. Phys.: Condens. Matter **15**, S1051 (2003).

[26] M. Sampoli, P. Benassi, R. Eramo, L. Angelani, and G. Ruocco, J. Phys.: Condens. Matter **15**, S1227 (2003).

[27] S. Sastry, N. Deo, and S. Franz, Phys. Rev. E **64**, 016305 (2001).

[28] G. Parisi, cond-mat/0301282 (unpublished); M. Mézard, G. Parisi, and A. Zee, cond-mat/9906135 (unpublished).

[29] G. Fagas, V. I. Fal'ko, and C. J. Lambert, Physica B **263–264**, 136 (1999).

[30] S. K. Sarkar, G. S. Matharoo, and A. Pandey, Phys. Rev. Lett. **92**, 215503 (2004).

[31] M. L. Mehta, *Random Matrices* (Academic Press, New York, 1991).

[32] T. A. Brody, J. Flores, J. B. French, P. A. Mello, A. Pandey, and S. S. M. Wong, Rev. Mod. Phys. **53**, 385 (1981); O. Bohigas and M. J. Giannoni, in *Mathematical and Computational Methods in Nuclear Physics, Proceedings of the Sixth Granada Workshop, Granada, Spain, 1983*, Lecture Notes in Physics Vol. 209 (Springer, Berlin, 1984); T. Guhr, A. Müller-Groeling and H. A. Weidenmüller, Phys. Rep. **299**, 189 (1998); C. W. J. Beenakker, Rev. Mod. Phys. **69**, 731 (1997).

[33] O. Bohigas, R. U. Haq, and A. Pandey, Phys. Rev. Lett. **54**, 1645 (1985).

[34] A. I. Chumakov, I. Sergueev, U. van Bürck, W. Schirmacher, T. Asthalter, R. Rüffer, O. Leupold, and W. Petry, Phys. Rev. Lett. **92**, 245508 (2004).

[35] F. Cleri and V. Rosato, Phys. Rev. B **48**, 22 (1993); A. P. Sutton and J. Chen, Philos. Mag. Lett. **61**, 139 (1990).

[36] R. P. Gupta, Phys. Rev. B **23**, 6265 (1981); V. Rosato, M. Guillope, and B. Legrand, Philos. Mag. A **59**, 321 (1989).

[37] J. S. Hunjan, S. Sarkar, and R. Ramaswamy, Phys. Rev. E **66**, 046704 (2002).

[38] I. L. Garzón and A. Posada-Amarillas, Phys. Rev. B **54**, 11796 (1996); J. P. K. Doye and D. J. Wales, Science **271**, 484 (1996).

[39] A. Fielicke, A. Kirilyuk, C. Ratsch, J. Behler, M. Scheffler, G. von Helden, and G. Meijer, Phys. Rev. Lett. **93**, 023401 (2004).